PLOS ONE

RESEARCH ARTICLE

COVID-19 pneumonia: Prediction of patient outcome by CT-based quantitative lung parenchyma analysis combined with laboratory parameters

Thuy D. Do[1,2], Stephan Skornitzke[1], Uta Merle[3], Maximilian Kittel[4], Stefan Hofbaur[5], Claudius Melzig[1,2], Hans-Ulrich Kauczor[1,2,6], Mark O. Wielpütz[1,2,6], Oliver Weinheimer[1,2]*

1 Clinic for Diagnostic and Interventional Radiology (DIR), University Hospital Heidelberg, Heidelberg, Germany, **2** Translational Lung Research Center Heidelberg (TLRC), German Center for Lung Research (DZL), Heidelberg, Germany, **3** Department of Internal Medicine IV (Gastroenterology and Infectious Disease), University Hospital Heidelberg, Heidelberg, Germany, **4** Institute for Clinical Chemistry, Medical Faculty Mannheim of Heidelberg University, Mannheim, Germany, **5** Clinic for Gastroenterology and Nephrology, Landshut Hospital, Landshut, Germany, **6** Department of Diagnostic and Interventional Radiology with Nuclear Medicine, Thoraxklinik, University Hospital Heidelberg, Heidelberg, Germany

* oliver.weinheimer@med.uni-heidelberg.de

OPEN ACCESS

Citation: Do TD, Skornitzke S, Merle U, Kittel M, Hofbaur S, Melzig C, et al. (2022) COVID-19 pneumonia: Prediction of patient outcome by CT-based quantitative lung parenchyma analysis combined with laboratory parameters. PLoS ONE 17(7): e0271787. https://doi.org/10.1371/journal.pone.0271787

Editor: Yann Benetreau, Public Library of Science, UNITED STATES

Received: January 22, 2021

Accepted: July 7, 2022

Published: July 29, 2022

Data Availability Statement: All relevant data are within the manuscript and its Supporting Information files.

Funding: The author(s) received no specific funding for this work.

Competing interests: Dr. Stephan Skornitzke has ownership interests in investment funds containing stock of healthcare companies. Dr. Thuy Duong Do was supported by a grant from the Medical Faculty of the University of Heidelberg. Prof. Dr. Mark O.

Abstract

Objectives

To evaluate the prognostic value of fully automatic lung quantification based on spectral computed tomography (CT) and laboratory parameters for combined outcome prediction in COVID-19 pneumonia.

Methods

CT images of 53 hospitalized COVID-19 patients including virtual monochromatic reconstructions at 40-140keV were analyzed using a fully automated software system. Quantitative CT (QCT) parameters including mean and percentiles of lung density, fibrosis index ($FIBI_{-700}$, defined as the percentage of segmented lung voxels $\geq$-700 HU), quantification of ground-glass opacities and well-aerated lung areas were analyzed. QCT parameters were correlated to laboratory and patient outcome parameters (hospitalization, days on intensive care unit, invasive and non-invasive ventilation).

Results

Best correlations were found for laboratory parameters LDH (r = 0.54), CRP (r = 0.49), Procalcitonin (r = 0.37) and partial pressure of oxygen (r = 0.35) with the QCT parameter 75th percentile of lung density. LDH, Procalcitonin, 75th percentile of lung density and $FIBI_{-700}$ were the strongest independent predictors of patients' outcome in terms of days of invasive ventilation. The combination of LDH and Procalcitonin with either 75th percentile of lung density or $FIBI_{-700}$ achieved a r^2 of 0.84 and 1.0 as well as an area under the receiver operating characteristic curve (AUC) of 0.99 and 1.0 for the prediction of the need of invasive ventilation.

Wielpütz receives funding from Boehringer Ingelheim and Vertex Pharma, outside the submitted work. This does not alter our adherence to PLOS ONE policies on sharing data and materials.

Abbreviations: BGA, Blood gas analysis; COVID-19, Coronavirus disease 2019; CK, Creatine kinase; CRP, C-reactive protein; CT, Computed tomography; HU, Hounsfield Unit; ICU, Intensive care unit; IL-6, Interleukine-6; IMC, Intermediate care; LDH, Lactate dehydrogenase; RT-PCR, Real-time reverse transcription polymerase chain reaction; SARS-CoV-2, Severe acute respiratory syndrome coronavirus 2.

Conclusions

QCT parameters in combination with laboratory parameters could deliver a feasible prognostic tool for the prediction of invasive ventilation in patients with COVID-19 pneumonia.

Introduction

Coronavirus disease 2019 (COVID-19) was declared a pandemic by the World Health Organization on March 11th 2020 and has caused 27,339,132 infections and 892,648 deaths worldwide (as of September 8th 2020) according to the Johns Hopkins dashboard [1]. The lung is the predominant organ affected by the disease presenting as pneumonia with rapid progression to severe respiratory distress syndrome requiring intensive care unit admission in up to 32% of cases [2, 3]. CT plays an essential role in early detection of pneumonia and can identify typical radiological patterns found in COVID-19: from ground-glass opacities in early stages to consolidation with a predominant peripheral distribution up to two weeks after disease onset [4, 5]. Sensitivities of chest CT for identification of COVID-19 of up to 98% have been reported and were shown to be superior to real-time polymerase chain reaction (RT-PCR) with sensitivities of 71% [6]. However, CT appearance is considered to be non-specific, though Bai et al. reported CT-specificity of 93% for distinguishing COVID-19 from other viral pneumonias [7]. Good correlations of CT features with severity of the disease and clinical parameters have been shown, e.g. 23–50% lung involvement with critical illness requiring ICU care [8–10].

Fully automatic quantification of structural lung disease, i.e. quantitative CT (QCT), has already been used as a feasible method for the evaluation of emphysema, airways disease, interstitial lung disease or atelectasis in large study population [11–17]. Many studies have shown laboratory parameters correlate with the degree of lung involvement in COVID-19 pneumonia using semi-quantitative or quantitative scoring, especially inflammation parameters such as C-reactive protein, D-dimer, interleukin-6, blood count or blood gas analysis [10, 18, 19].

We hypothesize that lung density changes such as ground-glass opacities and consolidation in COVID-19 pneumonia can be captured by QCT and that the extent of these changes may be not only related to disease severity, but also allows for prognostication in combination with clinical and laboratory parameters at the time of hospital admission.

Therefore, the aim of this study was to quantify early and advanced signs of COVID-19 pneumonia by attenuation-based QCT and correlate QCT parameters as well as established laboratory parameters with patient outcome.

Material and methods

Study design and patient recruitment

This retrospective exploratory single center study was performed according to the Declaration of Helsinki. Ethical approval was obtained from the local ethical review board of the Medical Faculty University Hospital Heidelberg with approval number S-293/2020. The need for written informed consent was waived.

Clinical data selection and study design

Eighty-six patients were referred to our institution with symptoms of COVID-19 pneumonia and admitted to the isolation ward between March and May 2020 were retrieved from the radiological information system (Centricity RIS, GE Healthcare) and eligible for study

inclusion. Inclusion criteria were one positive RT-PCR test and at least one chest CT with abnormal findings. 17 patients with other causes for pneumonia, such as influenza A and B proven by RT-PCR, were excluded. 15 patients were excluded due to contrast media application. One patient with streaking artifacts due to extensive breathing artifacts was excluded. To ensure comparability and homogeneity of acquisition settings, only 53 patients examined with the same CT-scanner and non-contrast enhanced acquisition protocol were included into the study.

Patients' clinical information and laboratory parameters were obtained from the hospital information system (I.S.-H.*med., SAP). Clinical information included date of CT, symptoms, date of symptom onset, admission and duration of hospitalization/intermediate care/intensive care unit, need and duration of invasive and non-invasive ventilation. Laboratory parameters within 24 hours of the CT included creatine kinase (CK), leucocytes, thrombocytes, neutrophile granulocytes, eosinophil granulocytes, lymphocytes, lactate dehydrogenase (LDH), C-reactive protein (CRP), interleukine-6 (IL-6), Procalcitonin and coagulation parameters. Blood gas analysis parameters i.e. partial pressure of oxygen (PaO2), partial pressure of carbon dioxide (PaCO2), pH-value, base deficit/excess and lactate were also retrieved. Only blood gas analysis that was closest to the time point of CT imaging with a maximum of 24 hours time interval was taken into account.

CT protocol, reconstruction and image postprocessing

Non-contrast enhanced chest CT was performed on a dual-layer detector spectral CT scanner (IQon, Philips). Patients were in supine position and acquisitions were obtained at end-inspiratory breath-hold achieving near total lung capacity and preventing atelectasis. Acquisition parameters were as follows: collimation 64 x 0.625 mm, tube potential 120 kV_p, automated tube current modulation, reference tube current 47 mAs, pitch 1.0, dose right index 9 and $CTDI_{vol}$ 3.8 mGy. Axial reconstructions with 1.5 mm slice thickness und 0.75 mm interval with lung kernel (YB) and soft tissue kernel (IMR1) were performed. In addition, pseudo-monoenergetic images from 40 to 140 keV in steps of 20 keV and reconstruction kernel B were generated using manufacturer's dedicated image postprocessing software (IntelliSpace, Philips).

Quantitative image analysis

Quantitative image analysis was performed with YACTA (version 2.9.0.31), a non-commercial, well-evaluated scientific software as previously described [11, 16, 17, 20–23]. YACTA segmented and analyzed the airway tree, the vessels and the lungs fully automatically. Ye, et al. described chest CT manifestation of COVID-19 in line with terms defined by the Fleischner Society such as ground-glass opacity, consolidation and crazy paving pattern [4]. We chose the following QCT parameters as COVID-19 markers:

1. Mean lung density (MLD), defined as the average CT values of all segmented lung voxels. The CT values are closely related to the lung density [24].
2. i^{th} percentile of the lung histogram, defined as the CT value such that i percent of the lung voxels are less than or equal to that CT value. In [22] is shown that percentiles might reflect changes in lung abnormalities.
3. Fibrosis index ($FIBI_{-700}$), defined as the percentage of the segmented lung voxels $\geq$ -700 HU, voxels labeled as vessel are excluded. This index is intended to describe the proportion of consolidations.

4. Ground-glass opacity index ($GGOI_{-800}$), defined as the percentage of the segmented lung voxels $\geq$−800 HU and <-700 HU. This index is intended to describe the proportion of GGO regions that can be seen as a precursor to consolidations.
5. Healthy lung index (HLI_{-700}), defined as the percentage of the segmented lung voxels $\geq$-950 HU and <-700 HU [18].
6. Wall%, defined as average of the quotient airway wall area and the total airway area for the whole segmented airway tree [20].
7. AWT-Pi10, defined as the square root of the airway wall area for a 'theoretical airway' with an internal perimeter of 10 mm [25].
8. Central and peripheral vessel volume. Therefore, the lung was divided into inner (core) and outer (in the rind) region, central vessels are located in the core region, peripheral vessels int the rind region [26].

Note, that the chosen $GGOI_{-800}$ interval is part of the HLI_{-700} interval, to identify whether this partial HU interval can provide additional information on an incipient COVID-19 disease. The image analysis was performed for the reconstructions with soft tissue kernel (IMR1), lung kernel(YB) and all six pseudo-monochromatic reconstructions (VMSI) from 40 to 140 keV (B).

Statistical analysis

Statistical analyses were performed using RStudio (R version 4.0.2). Pearson's correlation for linear correlation between QCT parameters of all different lung reconstructions (IMR1, YB, VMSI 40–140 keV B), laboratory values and interval scaled clinical outcome parameters were computed. For correlation of binary variables (invasive and non-invasive ventilation) with metric variables from QCT and laboratory parameters the pseudo r^2 (McFadden's r^2) was calculated. Multiple linear regression and logistic regression with backward, forward and bidirectional elimination was performed to achieve the best combination of laboratory, QCT and clinical parameters to predict different clinical endpoints. The Akaike Information Criterion (AIC) was used to identify the best model [27]. Furthermore, receiver operating curve (ROC) analysis was done and the area under the ROC curve (AUC) was calculated to determine the model performance of logistic regression analysis. The significance level for statistical testing was set at $p<0.05$, because of the exploratory nature of the study the Benjamini-Hochberg method was used for adjustment for multiple testing [28].

Results

Patient population

The mean age of the study population was 59.9 ±14 years and the patient collective comprised 19 females and 34 males (**Table 1**). Average time between onset of symptoms and initial CT imaging was 7.1 ± 4.9 days (median: 7.0 days). CT imaging was routinely performed on the first day of admission. Main initial symptoms were fever (88%), cough (81%), dyspnea (50%), diarrhea (35%), pain in the limbs (26%) and fatigue (24%). Among the 53 hospitalized patients with a CT scan five patients were admitted to an isolation ward and 48 patients on intermediate or intensive care unit. On average patients were hospitalized for 12.2 ± 6.8 days (median: 12.0 days) and spent 10.2 ±6.4 days (median: 8.0 days) on intermediate care or intensive care unit. Those who needed respiratory support were ventilated non-invasively for a mean of

Table 1. Characteristics of study population.

Characteristics of study population (n = 53)	Mean and SD
Age [years]	59.9 ± 14.0
Sex [n (%)]	
Female	19 (36%)
Male	34 (64%)
Length of hospitalization [days]	12.2 ± 6.8
Length patient care on ICU/ICM [days]	10.2 ± 6.4
Need for non-invasive ventilation [n (%)]	14 (26.4%)
Length of non-invasive ventilation [days]	5.3 ± 3.7
Need for invasive ventilation [n (%)]	11 (20.6%)
Length of invasive ventilation [days]	14.6 ± 9.6

https://doi.org/10.1371/journal.pone.0271787.t001

5.3 ± 3.7 days (median: 4 days; 15 patients) or invasively for 14.6 ±9.6 days (median: 14 days; 11 patients), respectively.

Laboratory testing

Laboratory studies with mean values and standard deviation (Table 2) demonstrated lymphopenia 0.83/nl (normal range: 1.0–4.8/nl); D-dimer was elevated 1.19 mg/dl (normal range <0.5 mg/dl); Additional parameters included thrombocytes, leucocytes and coagulation parameters (pTT, INR) were within the normal range. There was an increase of CRP 81.6 mg/l (normal range <5 mg/l) and LDH 391.28 (normal range <317 U/l). Pathologic blood gas analysis was noticeable in 14 cases (26%), from which in 11 cases were respiratory alkalosis and three cases of respiratory azidosis.

QCT analysis

All QCT parameters are shown in Table 3 and an example of automatic lung segmentation without manual correction is presented in Fig 1. We found only slight differences in the QCT parameters for the different reconstructions. In the following, we therefore focus only on the QCT results generated for IMR1 reconstructions, as we saw the best correlation between QCT and laboratory parameters there.

Table 2. Mean and standard deviation of the laboratory parameters of all 53 COVID-19 patients.

Laboratory parameter	Mean and SD of 53 patients	Normal range
Leucocytes	6.17 ± 3.02/nl	4-10/nl
Lymphocytes	0.83 ± 0.36/nl	1.0–4.8/nl
Neutrophilic granulocytes	4.81 ± 2.91/nl	1.8–7.7/nl
Eosinophilic granulocytes	0.44 ± 0.08/nl	<0.5/nl
Thrombocytes	209.38 ± 76.45/nl	150-440/nl
Lactate dehydrogenase	391.28 ± 128.94 U/l	<317 U/l
C-reactive protein	81.65 ± 82.05 mg/l	<5 mg/l
Interleukine-6	473.46 ± 296 pg/ml	<15 pg/ml
Procalcitonin	0.37 ± 1.30 ng/ml	<0.05 ng/ml
International Normalized Ratio	1.10 ± 0.25	<1.2
Prothrombin time	25.15 ± 3.56 s	<35 s
D-Dimer	1.19 ± 1.83 mg/l	<0.5 mg/l
Creatine kinase	168.47 ± 213.73 U/l	<190 U/l

https://doi.org/10.1371/journal.pone.0271787.t002

Table 3. QCT parameters of 53 COVID-19 patients in the soft kernel images IMR1.

QCT parameters	Mean and SD of 53 patients
Mean lung density	-681.19 ± 78.30 HU
80th percentile lung density	-544.26 ± 167.59 HU
75th percentile lung density	-621.47 ± 158.52 HU
70th percentile lung density	-674.75 ± 144.18 HU
$FIBI_{-700}$	30.55 ± 14.47%
GGO_{-800}	16.35 ± 9.70%
HLI_{-700}	66.10 ± 15.01%
Wall%	52.59 ± 5.34%
AWT-Pi10	0.31 ± 0.13 mm
Central vessel volume	129.31 ± 67.12 cm^3
Peripheral vessel volume	31.23 ± 27.28 cm^3

https://doi.org/10.1371/journal.pone.0271787.t003

The mean lung density was -681.2 ±78.3 HU, the 75th percentile lung density -621.5 ±158.5 HU, the mean of $FIBI_{-700}$ was 30.6 ±14.47%, $GGOI_{-800}$ was 16.4 ±9.7% and HLI_{-700} 66.1 ±15.0%. Percentage of airwall thickness was 0.31 ±5.34% and AWT-Pi-10 0.31 ± 0.13 mm. Central and peripheral vessel volume were 129.31 ± 67.12 cm^3 and 31.23 ± 27.28 cm^3, respectively.

Correlation analysis

Next, we correlated QCT parameters with laboratory work, blood gas analysis, body temperature, length of hospitalization and intermediate/intensive care unit and, length of invasive and non-invasive ventilation (**Fig 2 and S1 Appendix**). Comparing QCT parameters, the strongest correlation with laboratory and clinical parameters was observed for 70-80th lung percentiles (Pearson's r up to 0.54; $p<0.01$), HLI_{-700} ($r = -0.45$; $p<0.05$), mean lung density ($r = 0.43$; $p<0.05$), $FIBI_{-700}$ ($r = 0.45$; $p<0.05$) and central and peripheral vessel volume ($r = 0.49$ and 0.47, respectively; $p<0.05$) (**Figs 2 and 3**). Other QCT parameters e.g. $GGOI_{-800}$, Wall% and AWT-Pi10 showed lower or inversed correlations. Central vessel volume and peripheral vessel volume correlated strong positively with CRP ($r = 0.49–0.47$; $p<0.05$).

Strongest correlation between QCT parameters and laboratory data was observed for the soft tissue kernel IMR1 and slightly lower correlations were observed for the lung kernel YB (S2 Appendix) and virtual monoenergetic images 40–140 keV (S3-S8 Appendices).

Among laboratory parameters LDH ($r = 0.54$; $p<0.01$), CRP ($r = 0.49$; $p<0.05$), Procalcitonin ($r = 0.37$; $p>0.05$), and partial pressure of oxygen ($r = 0.35$; $p>0.05$) demonstrated the highest correlation coefficients with quantitative lung segmentation parameters such as 70th or 75th lung percentiles.

Pseudo r^2 was calculated for correlation of binary outcome parameters with laboratory and QCT parameters (**Fig 4**). Highest correlation of McFadden pseudo r^2 for whether patients were invasively or non-invasively ventilated was 0.47 for LDH and 0.41 for Procalcitonin. Length of hospitalization correlated with QCT percentiles of lung density ($r^2 = 0.14$, $p<0.01$). Length of invasive ventilation, non-invasive ventilation and days on intensive and intermediate care unit showed the highest correlation with partial oxygen pressure ($r^2 = 0.45$; $p<0.001$) and LDH (McFadden pseudo $r^2 = 0.47$) when evaluating laboratory parameters and with 70-80th percentile lung density (McFadden pseudo $r^2 = 0.31$) when evaluating quantitative lung segmentation parameters.

The backward elimination technique led to the best multiple linear regression model for the prediction of days of invasive ventilation according to the Akaike information criterion (AIC) leading to an adjusted r^2 of 0.72 with a p-value of 8.63e-10, detailed results see in S9 Appendix.

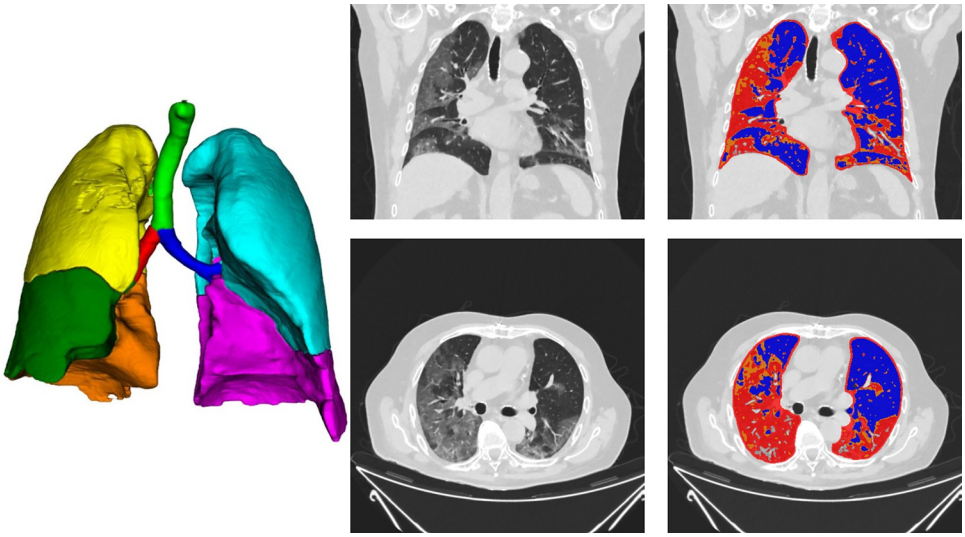

Fig 1. The YACTA software performed a fully automatic segmentation of airways, vessels and lung parenchyma of an 84y/o male with extensive lung infiltrates who received high-flow oxygen therapy and invasive ventilation. In the course of the disease he developed renal insufficiency, septic shock and died 21 days after symptom onset and 8 days after hospital admission. Consolidations are shown in red, ground-glass opacities in orange, healthy lung in blue, vessel voxels in grey are excluded. The 3D rendering shows the lung segmentation with their segmented lobes in different colors, in the statistical evaluation the lung parenchyma was considered as a whole.

https://doi.org/10.1371/journal.pone.0271787.g001

Combined prediction model

The predictive value of QCT and laboratory parameters for the necessity of invasive ventilation was investigated. ROC analysis was applied and the AUC was calculated to determine model performance. AUC value for ROC analysis based on simple logistic regression was 84.2% for

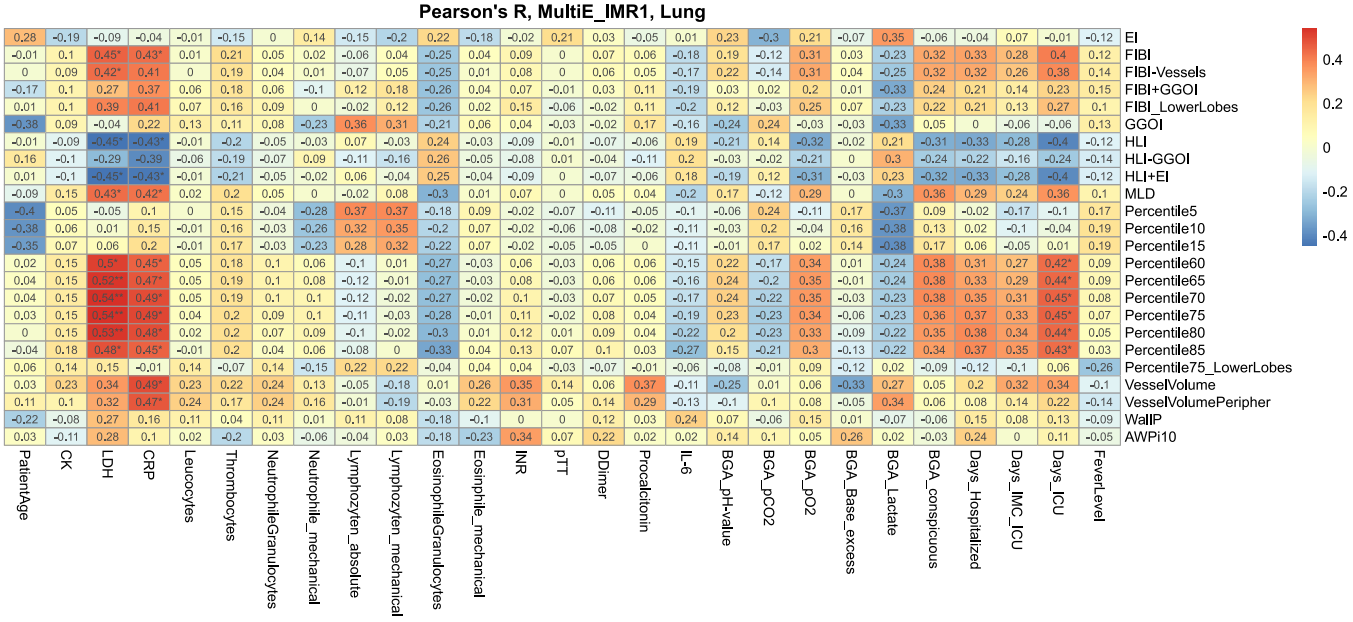

Fig 2. Heat map of Pearson's correlation between QCT lung segmentation (y-axis) and laboratory parameters and clinical outcome (x-axis). Significant codes: *** $p < 0.001$ / ** $p < 0.01$ / * $p < 0.05$.

https://doi.org/10.1371/journal.pone.0271787.g002

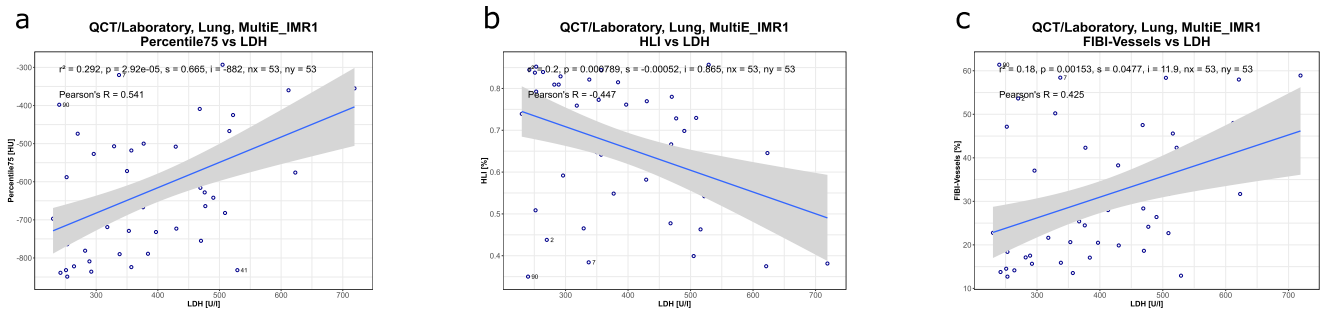

Fig 3. Correlations between LDH and QCT parameters with highest Pearson's r for 75th lung percentile in comparison to HLI$_{-700}$ and FIBI$_{-700}$.

https://doi.org/10.1371/journal.pone.0271787.g003

FIBI$_{-700}$ (McFadden pseudo $r^2 = 0.21$) and the best threshold delivered a true positive percentage (TPP, sensitivity) of 100% and a false positive percentage (FPP, 1-specificity) of 31%. 75th lung percentile parameter summed up to an AUC of 87.4% ($r^2 = 0.31$, TPP = 100%, FPP = 31%). AUC values for LDH were 91.5% ($r^2 = 0.47$, TPP = 82%, FPP = 14%) and for Procalcitonin 88.6% ($r^2 = 0.37$, TPP = 82%, FPP = 14%) for (Fig 5).

Backward elimination technique was used to identify the best multiple logistic regression model. The combination of FIBI$_{-700}$ with LDH and Procalcitonin achieved an AUC of 100% ($r^2 = 1$, TPP = 100%, FPP = 0%). The combination of 75th percentile lung density with LDH and Procalcitonin yielded an AUC of 99.4% ($r^2 = 0.84$, TPP = 100%, FPP = 5%, Fig 6).

Discussion

The aim of the study was to correlate the outcome of hospitalized patients with COVID-19 pneumonia with initial laboratory and imaging findings to identify predictive markers for disease progress. Correlations of initial QCT parameters of COVID-19 pneumonia with clinical parameters, such as days on intensive and/or intermediate care unit, and laboratory parameters, e.g. LDH, CRP, Procalcitonin and blood gas analysis, were observed. Thus, initial CT and laboratory testing could aid to stratify patient treatment and indicate patients might require closer monitoring at the time of hospital admission. Taken together, both could help to find solutions to provide cancer patients with better care [29, 30]. We showed that laboratory parameters Procalcitonin and LDH as well as QCT parameters FIBI$_{-700}$ and 75th percentile of lung density are predictors for the need for invasive ventilation. The combination of QCT parameters and laboratory work shows superior results for the prediction of the necessity of invasive ventilation. Though blood gas analysis and many other laboratory parameters were

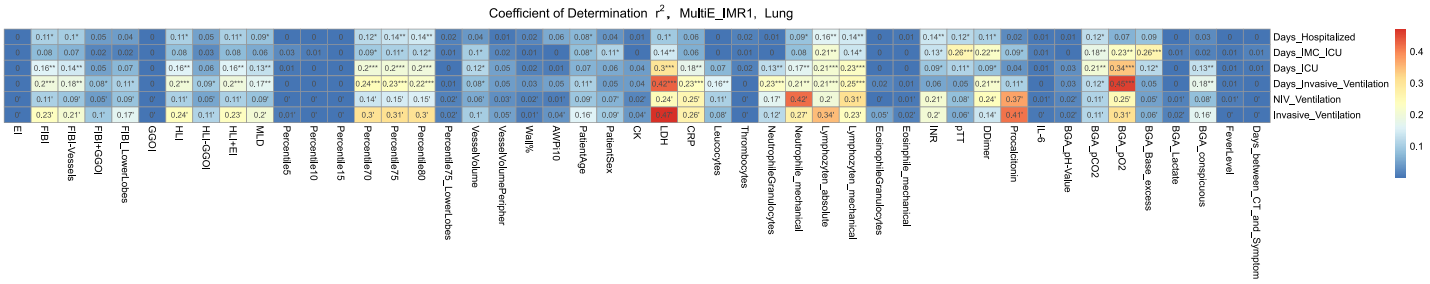

Fig 4. Heat map of coefficient of determination r^2 for the correlation of outcome parameters with laboratory and QCT parameters. For binary outcome parameters (NIV_Ventilation and Invasive_Ventilation) the Mc Fadden pseudo r^2 was calculated, there is no p-value to specify for this value. Signif. codes: *** $p < 0.001$ / ** $p < 0.01$ / * $p < 0.05$ / ' no p-value available.

https://doi.org/10.1371/journal.pone.0271787.g004

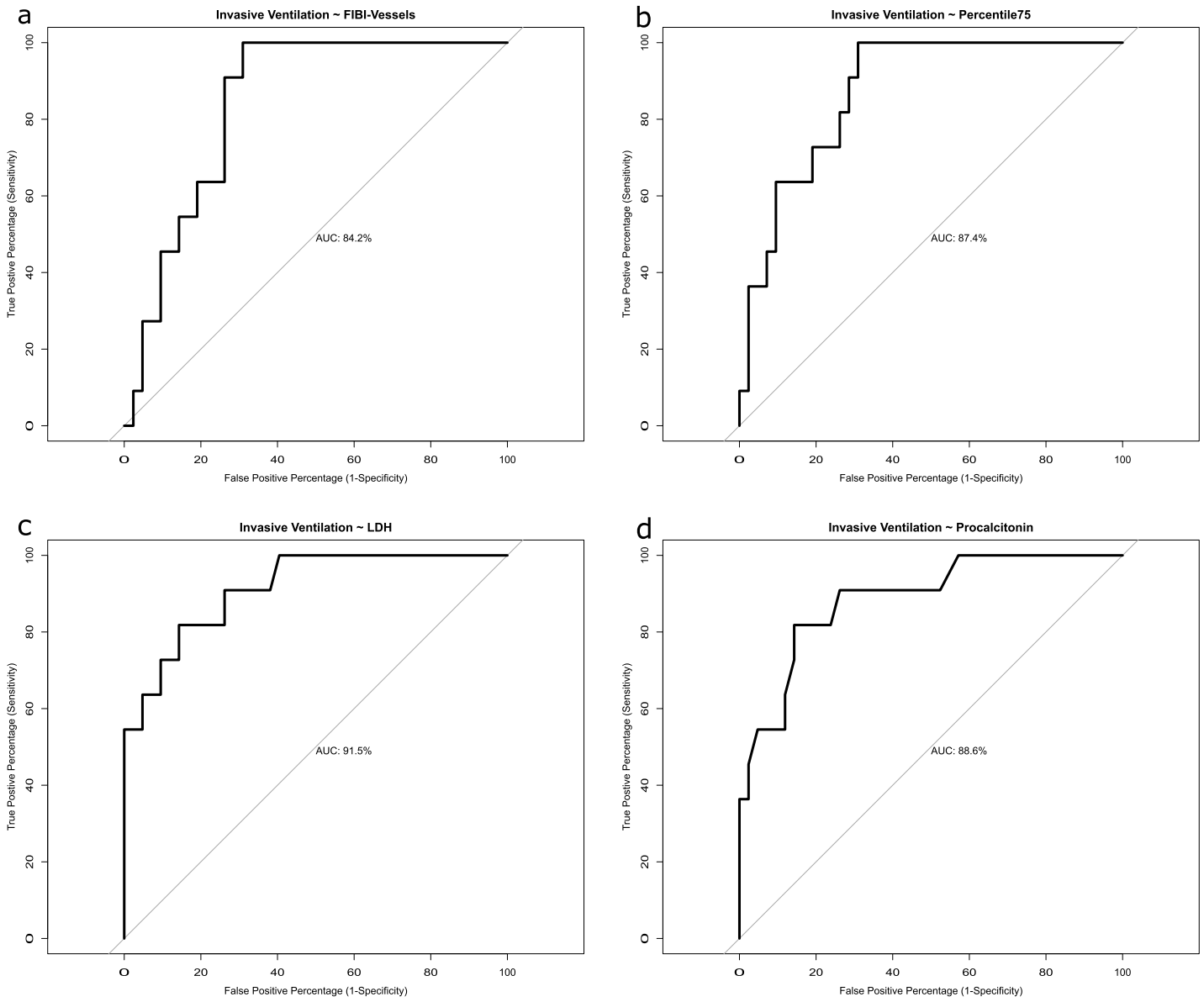

Fig 5. ROC curves of invasive ventilation QCT parameters alone with $FIBI_{-700}$ (a) vs. 75^{th} percentile lung density (b) vs. LDH (c) vs. Procalcitonin (d).

https://doi.org/10.1371/journal.pone.0271787.g005

taken into account for establishing a prediction score, only Procalcitonin and LDH showed significant results for establishing a prognostic score. Either a combination calculated from 75^{th} percentile of lung density, Procalcitonin and LDH or from $FIBI_{-700}$, Procalcitonin and LDH could be used to estimate the need for invasive ventilation.

Contrary to expectations, D-Dimer was only slightly elevated and did not show high correlations to any morphological lung segmentation parameters. This might be explained by the fact that in early stages of the diseases D-Dimer elevation is associated with inflammation and prothrombotic state and embolism are seen in ICU patients or patients with critical illness only when D-Dimer is markedly elevated [31]. Moreover, preventive anticoagulation is not recommended for COVID-19 for outpatients and low molecular weight heparin or unfractionated heparin may be given in hospitalized patients with severe illness [32, 33]. Another factor

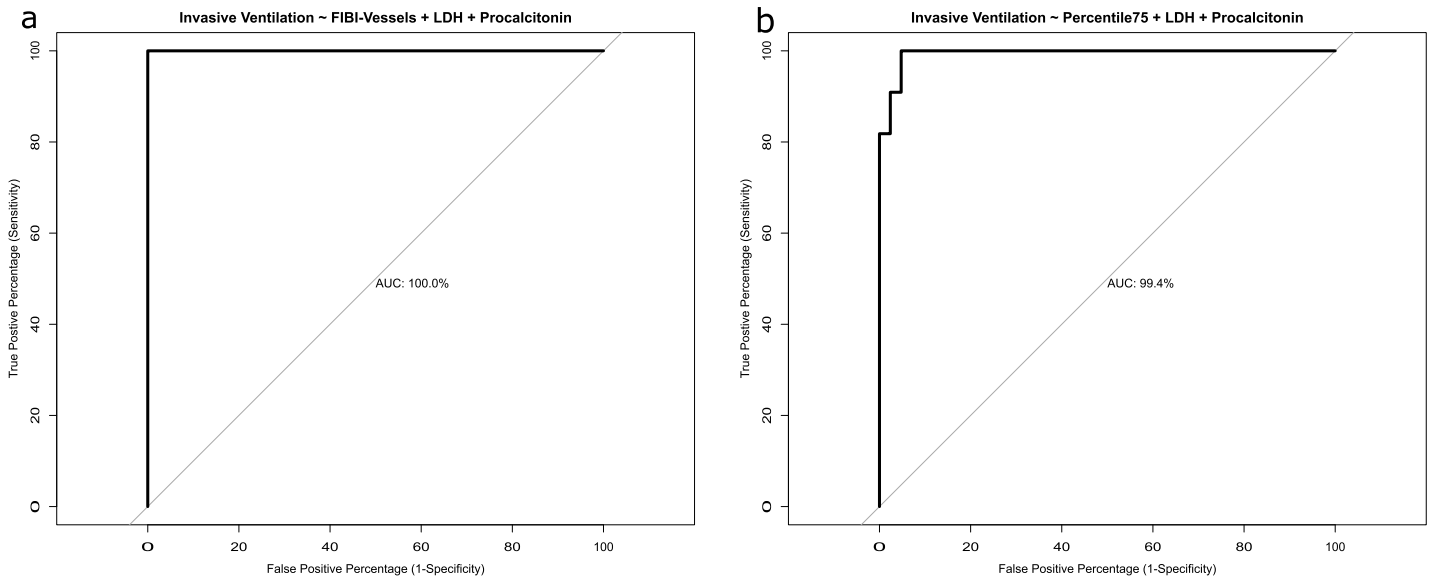

Fig 6. ROC curves for invasive ventilation consisting of the combination of QCT and laboratory work: $FIBI_{-700}$, LDH and Procalcitonin; (b) 75^{th} percentile lung density, LDH and Procalcitonin.

https://doi.org/10.1371/journal.pone.0271787.g006

might be using non-contrast chest scans which could exclude patients with a severe disease manifestation.

Colombi et al. proposed the usage of well-aerated lung as a parameter to predict outcome. Unfortunately, no additional QCT parameters were examined and thus potential tools for prognostication may be missed [34]. However, the method used in their study still required manual adjustments, which might limit its upscaling to a larger study population. Moreover, in this study the approach included the 75^{th} percentile of lung density, $FIBI_{-700}$ and normally-aerated lung proportion which showed comparable correlations with clinical parameters and outcome parameters. However, only $FIBI_{-700}$ in combination with LDH and Procalcitonin achieved an AUC of 100%. Wall% and AWT-Pi10 did not correlate well with laboratory parameters, as the pulmonary manifestations focuses on the lung parenchyma. In line with previous studies dilated vessel volumes on non-enhanced CT images has been reported and might be explained by small pulmonary embolism or paradoxical increase of blood flow [35, 36].

Several approaches have been made for automated or artificial intelligence-based lung segmentation in COVID-19 diseases to predict adverse outcome,ARDS only or correlation of lung segmentation with laboratory works, but did not use a multifactorial approach [22, 34, 37–39]. Park et al. have performed the first multifactorial approach to evaluate prognostic implication of lung segmentation and laboratory work, especially CRP, on outcome parameters [40]. However, manual adjustment was performed for the lung segmentation using commercially available software such as modifying parenchymal segmentation and exclusion of parenchymal lesions (honeycombing, bronchiectasis, pleural effusion and others). Our approach offers a fully-automated segmentation with an openly available algorithm without any further manual adjustments, as the threshold chosen already excludes those parenchymal lesions as mentioned above. The method has been used for different CT devices in previous studies and offers the opportunity for upscaling to a lager or nationwide population.

Gattinoni et al. suggest to adapt the ventilation according to the lung weight by differentiating them in low and high lung weight [41]. Fully automated segmentation of the lung might

facilitate the decision for the mode of ventilation and should be the subject of further investigations.

CT images reconstructed with the soft tissue kernel showed better correlations with laboratory and clinical parameters than the lung kernel or VMSI, which is in line with recommendations for lung segmentation of previous studies [42, 43]. All six VMSI reconstructions and lung kernel were slightly inferior to the soft tissue kernel in CT without contrast agent in this study. However, VMSI might be useful combined with contrast agent in patients with severe symptoms in advanced disease stage, especially with COVID-19 to detect associated thromboembolic complications [44, 45].

The most important limitation of the study was the modest number of patients and the retrospective nature of the study. Our results require further verification in a prospective trial. However, only patients hospitalized with a positive SARS-COV2 test confirmed by PCR were included and all patients received the same CT acquisition protocols at the same CT device. In general, the low number of included patients might be attributed to the overall low infection numbers in Germany, especially in this geographical region, at the time of the study. The segmentation algorithm has been employed for previous studies with different CT devices. Based on previous results, we estimate that the fully automatic segmentation can be transferred to a large multicentric cohort on a nationwide level with acceptable effort, provided that a national platform for images and clinical data is established. A wide range of laboratory parameters and gas blood analysis were included into the correlation analysis and prediction score establishment, and laboratory work was not standardized with sporadically missing values.

Conclusion

An independent correlation with clinical outcome parameters for COVID-19 could be shown for a wide range of laboratory parameters, with strongest correlations for CRP, Procalcitonin and LDH.

QCT parameters 70^{th}-80^{th} percentile of lung density and $FIBI_{-700}$ correlated best with clinical parameters and outcome. Fully QCT and laboratory testing are independently predictive factor for invasive ventilation. However, Procalcitonin and LDH in combination either with the 75^{th} percentile of lung density or $FIBI_{-700}$ achieved highest prognostic value for invasive ventilation derived from initial CT imaging.

Supporting information

S1 Appendix. Heat map of all QCT lung segmentation, laboratory and clinical outcome parameters.
(EPS)

S2 Appendix. Heat map of Pearson's correlation for lung kernel.
(EPS)

S3 Appendix. Heat map of Pearson's correlation for virtual monochromatic reconstruction at 140 keV.
(EPS)

S4 Appendix. Heat map of Pearson's correlation for virtual monochromatic reconstruction at 120 keV.
(EPS)

S5 Appendix. Heat map of Pearson's correlation for virtual monochromatic reconstruction at 100 keV.
(EPS)

S6 Appendix. Heat map of Pearson's correlation for virtual monochromatic reconstruction at 80 keV.
(EPS)

S7 Appendix. Heat map of Pearson's correlation for virtual monochromatic reconstruction at 60 keV.
(EPS)

S8 Appendix. Heat map of Pearson's correlation for virtual monochromatic reconstruction at 40 keV.
(EPS)

S9 Appendix. Result of best multiple linear regression model of QCT and laboratory parameter with clinical outcome parameters.
(DOCX)

Author Contributions

Conceptualization: Thuy D. Do, Stephan Skornitzke, Maximilian Kittel, Claudius Melzig, Oliver Weinheimer.

Data curation: Thuy D. Do.

Formal analysis: Thuy D. Do.

Investigation: Thuy D. Do, Stefan Hofbaur, Oliver Weinheimer.

Methodology: Thuy D. Do, Stephan Skornitzke, Uta Merle, Maximilian Kittel, Claudius Melzig, Oliver Weinheimer.

Project administration: Hans-Ulrich Kauczor.

Resources: Hans-Ulrich Kauczor, Mark O. Wielpütz.

Software: Oliver Weinheimer.

Supervision: Uta Merle, Stefan Hofbaur, Claudius Melzig, Hans-Ulrich Kauczor, Mark O. Wielpütz.

Validation: Oliver Weinheimer.

Visualization: Oliver Weinheimer.

Writing – original draft: Thuy D. Do, Stephan Skornitzke, Oliver Weinheimer.

Writing – review & editing: Stephan Skornitzke, Uta Merle, Maximilian Kittel, Stefan Hofbaur, Claudius Melzig, Hans-Ulrich Kauczor, Mark O. Wielpütz.

References

1. John Hopkins University. Coronavirus COVID-19 global cases for the center for systems science and engineering. https://coronavirus.jhu.edu/map.html (accessed 08 Sept 2020).
2. Wu Z, McGoogan JM. Characteristics of and Important Lessons From the Coronavirus Disease 2019 (COVID-19) Outbreak in China: Summary of a Report of 72314 Cases From the Chinese Center for Disease Control and Prevention. JAMA. 2020. https://doi.org/10.1001/jama.2020.2648 PMID: 32091533

3. Huang C, Wang Y, Li X, Ren L, Zhao J, Hu Y, et al. Clinical features of patients infected with 2019 novel coronavirus in Wuhan, China. Lancet. 2020; 395(10223):497–506. https://doi.org/10.1016/S0140-6736(20)30183-5 PMID: 31986264
4. Pan F, Ye T, Sun P, Gui S, Liang B, Li L, et al. Time Course of Lung Changes On Chest CT During Recovery From 2019 Novel Coronavirus (COVID-19) Pneumonia. Radiology. 2020:200370.
5. Bernheim A, Mei X, Huang M, Yang Y, Fayad ZA, Zhang N, et al. Chest CT Findings in Coronavirus Disease-19 (COVID-19): Relationship to Duration of Infection. Radiology. 2020:200463. https://doi.org/10.1148/radiol.2020200463 PMID: 32077789
6. Fang Y, Zhang H, Xie J, Lin M, Ying L, Pang P, et al. Sensitivity of Chest CT for COVID-19: Comparison to RT-PCR. Radiology. 2020:200432. https://doi.org/10.1148/radiol.2020200432 PMID: 32073353
7. Bai HX, Hsieh B, Xiong Z, Halsey K, Choi JW, Tran TML, et al. Performance of radiologists in differentiating COVID-19 from viral pneumonia on chest CT. Radiology. 2020:200823.
8. Xiong Y, Sun D, Liu Y, Fan Y, Zhao L, Li X, et al. Clinical and High-Resolution CT Features of the COVID-19 Infection: Comparison of the Initial and Follow-up Changes. Invest Radiol. 2020. https://doi.org/10.1097/RLI.0000000000000674 PMID: 32134800
9. Leonardi A, Scipione R, Alfieri G, Petrillo R, Dolciami M, Ciccarelli F, et al. Role of computed tomography in predicting critical disease in patients with covid-19 pneumonia: A retrospective study using a semiautomatic quantitative method. Eur J Radiol. 2020; 130:109202. https://doi.org/10.1016/j.ejrad.2020.109202 PMID: 32745895
10. Li Z, Zhong Z, Li Y, Zhang T, Gao L, Jin D, et al. From community-acquired pneumonia to COVID-19: a deep learning-based method for quantitative analysis of COVID-19 on thick-section CT scans. Eur Radiol. 2020. https://doi.org/10.1007/s00330-020-07042-x PMID: 32683550
11. Konietzke P, Wielputz MO, Wagner WL, Wuennemann F, Kauczor HU, Heussel CP, et al. Quantitative CT detects progression in COPD patients with severe emphysema in a 3-month interval. Eur Radiol. 2020.
12. Boehme S, Toemboel FPR, Hartmann EK, Bentley AH, Weinheimer O, Yang Y, et al. Detection of inspiratory recruitment of atelectasis by automated lung sound analysis as compared to four-dimensional computed tomography in a porcine lung injury model. Crit Care. 2018; 22(1):50. https://doi.org/10.1186/s13054-018-1964-6 PMID: 29475456
13. Kauczor HU, Heussel CP, Herth FJ. Longitudinal quantitative low-dose CT in COPD: ready for use? Lancet Respir Med. 2013; 1(2):95–6. https://doi.org/10.1016/S2213-2600(13)70011-0 PMID: 24429077
14. Kauczor HU, Wielputz MO, Jobst BJ, Weinheimer O, Gompelmann D, Herth FJF, et al. Computed Tomography Imaging for Novel Therapies of Chronic Obstructive Pulmonary Disease. J Thorac Imaging. 2019; 34(3):202–13. https://doi.org/10.1097/RTI.0000000000000378 PMID: 30550404
15. Jacob J, Bartholmai BJ, Rajagopalan S, van Moorsel CHM, van Es HW, van Beek FT, et al. Predicting Outcomes in Idiopathic Pulmonary Fibrosis Using Automated Computed Tomographic Analysis. Am J Respir Crit Care Med. 2018; 198(6):767–76. https://doi.org/10.1164/rccm.201711-2174OC PMID: 29684284
16. Jobst BJ, Weinheimer O, Buschulte T, Trauth M, Tremper J, Delorme S, et al. Longitudinal airway remodeling in active and past smokers in a lung cancer screening population. Eur Radiol. 2019; 29(6):2968–80. https://doi.org/10.1007/s00330-018-5890-4 PMID: 30552475
17. Jobst BJ, Weinheimer O, Trauth M, Becker N, Motsch E, Gross ML, et al. Effect of smoking cessation on quantitative computed tomography in smokers at risk in a lung cancer screening population. Eur Radiol. 2018; 28(2):807–15. https://doi.org/10.1007/s00330-017-5030-6 PMID: 28884215
18. Francone M, Iafrate F, Masci GM, Coco S, Cilia F, Manganaro L, et al. Chest CT score in COVID-19 patients: correlation with disease severity and short-term prognosis. Eur Radiol. 2020; 30(12):6808–17. https://doi.org/10.1007/s00330-020-07033-y PMID: 32623505
19. Chen LD, Zhang ZY, Wei XJ, Cai YQ, Yao WZ, Wang MH, et al. Association between cytokine profiles and lung injury in COVID-19 pneumonia. Respir Res. 2020; 21(1):201. https://doi.org/10.1186/s12931-020-01465-2 PMID: 32727465
20. Weinheimer O, Achenbach T, Bletz C, Duber C, Kauczor H-U, Heussel CP. About objective 3-d analysis of airway geometry in computerized tomography. IEEE transactions on medical imaging. 2007; 27(1):64–74.
21. Konietzke P, Weinheimer O, Wielputz MO, Savage D, Ziyeh T, Tu C, et al. Validation of automated lobe segmentation on paired inspiratory-expiratory chest CT in 8–14 year-old children with cystic fibrosis. PLoS One. 2018; 13(4):e0194557. https://doi.org/10.1371/journal.pone.0194557 PMID: 29630630
22. Colombi D, Dinkel J, Weinheimer O, Obermayer B, Buzan T, Nabers D, et al. Visual vs Fully Automatic Histogram-Based Assessment of Idiopathic Pulmonary Fibrosis (IPF) Progression Using Sequential

Multidetector Computed Tomography (MDCT). PLoS One. 2015; 10(6):e0130653. https://doi.org/10.1371/journal.pone.0130653 PMID: 26110421

23. Wielputz MO, Eichinger M, Weinheimer O, Ley S, Mall MA, Wiebel M, et al. Automatic airway analysis on multidetector computed tomography in cystic fibrosis: correlation with pulmonary function testing. J Thorac Imaging. 2013; 28(2):104–13. https://doi.org/10.1097/RTI.0b013e3182765785 PMID: 23222199

24. Kalender WA, Rienmuller R, Seissler W, Behr J, Welke M, Fichte H. Measurement of pulmonary parenchymal attenuation: use of spirometric gating with quantitative CT. Radiology. 1990; 175(1):265–8. https://doi.org/10.1148/radiology.175.1.2315492 PMID: 2315492

25. Grydeland TB, Dirksen A, Coxson HO, Pillai SG, Sharma S, Eide GE, et al. Quantitative computed tomography: emphysema and airway wall thickness by sex, age and smoking. Eur Respir J. 2009; 34 (4):858–65. https://doi.org/10.1183/09031936.00167908 PMID: 19324952

26. Nakano Y, Coxson HO, Bosan S, Rogers RM, Sciurba FC, Keenan RJ, et al. Core to rind distribution of severe emphysema predicts outcome of lung volume reduction surgery. Am J Respir Crit Care Med. 2001; 164(12):2195–9. https://doi.org/10.1164/ajrccm.164.12.2012140 PMID: 11751187

27. Akaike H. A new look at the statistical model identification. IEEE transactions on automatic control. 1974; 19(6):716–23.

28. Benjamini Y, Hochberg Y. Controlling the false discovery rate: a practical and powerful approach to multiple testing. Journal of the Royal statistical society: series B (Methodological). 1995; 57(1):289–300.

29. Fadavi P., Houshyari M., Yousefi Kashi A.S., Jarrahi A.M., Roshanmehr F., Broomand M.A., et al. Review on the Oncology Practice in the Midst of COVID-19 Crisis: The Challenges and Solutions, Asian Pac J Cancer Prev 22(1) (2021) 19–24. https://doi.org/10.31557/APJCP.2021.22.1.19 PMID: 33507674

30. Rakhsha A., Azghandi S., Taghizadeh-Hesary F. Decision on Chemotherapy Amidst COVID-19 Pandemic: a Review and a Practical Approach from Iran, Infect Chemother 52(4) (2020) 496–502. https://doi.org/10.3947/ic.2020.52.4.496 PMID: 33263246

31. Bikdeli B, Madhavan MV, Jimenez D, Chuich T, Dreyfus I, Driggin E, et al. COVID-19 and Thrombotic or Thromboembolic Disease: Implications for Prevention, Antithrombotic Therapy, and Follow-Up: JACC State-of-the-Art Review. J Am Coll Cardiol. 2020; 75(23):2950–73. https://doi.org/10.1016/j.jacc.2020.04.031 PMID: 32311448

32. Thachil J, Tang N, Gando S, Falanga A, Cattaneo M, Levi M, et al. ISTH interim guidance on recognition and management of coagulopathy in COVID-19. J Thromb Haemost. 2020; 18(5):1023–6. https://doi.org/10.1111/jth.14810 PMID: 32338827

33. Tang N, Li D, Wang X, Sun Z. Abnormal coagulation parameters are associated with poor prognosis in patients with novel coronavirus pneumonia. J Thromb Haemost. 2020; 18(4):844–7. https://doi.org/10.1111/jth.14768 PMID: 32073213

34. Colombi D, Bodini FC, Petrini M, Maffi G, Morelli N, Milanese G, et al. Well-aerated Lung on Admitting Chest CT to Predict Adverse Outcome in COVID-19 Pneumonia. Radiology. 2020; 296(2):E86–E96. https://doi.org/10.1148/radiol.2020201433 PMID: 32301647

35. Saba L, Sverzellati N. Is COVID Evolution Due to Occurrence of Pulmonary Vascular Thrombosis? J Thorac Imaging. 2020; 35(6):344–5. https://doi.org/10.1097/RTI.0000000000000530 PMID: 32349055

36. Raptis CA, Hammer MM, Henry TS, Hope MD, Schiebler ML, van Beek EJR. What Do We Really Know About Pulmonary Thrombosis in COVID-19 Infection? J Thorac Imaging. 2020; 35(6):341–3. https://doi.org/10.1097/RTI.0000000000000545 PMID: 32618808

37. Nishiyama A, Kawata N, Yokota H, Sugiura T, Matsumura Y, Higashide T, et al. A predictive factor for patients with acute respiratory distress syndrome: CT lung volumetry of the well-aerated region as an automated method. Eur J Radiol. 2020; 122:108748. https://doi.org/10.1016/j.ejrad.2019.108748 PMID: 31775082

38. Ni Q, Sun ZY, Qi L, Chen W, Yang Y, Wang L, et al. A deep learning approach to characterize 2019 coronavirus disease (COVID-19) pneumonia in chest CT images. Eur Radiol. 2020. https://doi.org/10.1007/s00330-020-07044-9 PMID: 32617690

39. Li L, Qin L, Xu Z, Yin Y, Wang X, Kong B, et al. Using Artificial Intelligence to Detect COVID-19 and Community-acquired Pneumonia Based on Pulmonary CT: Evaluation of the Diagnostic Accuracy. Radiology. 2020; 296(2):E65–E71. https://doi.org/10.1148/radiol.2020200905 PMID: 32191588

40. Park B, Park J, Lim JK, Shin KM, Lee J, Seo H, et al. Prognostic Implication of Volumetric Quantitative CT Analysis in Patients with COVID-19: A Multicenter Study in Daegu, Korea. Korean J Radiol. 2020. https://doi.org/10.3348/kjr.2020.0567 PMID: 32767868

41. Gattinoni L, Quintel M, Marini JJ. "Less is More" in mechanical ventilation. Intensive Care Med. 2020; 46(4):780–2. https://doi.org/10.1007/s00134-020-05981-z PMID: 32162029

42. Newell JD Jr., Sieren J, Hoffman EA. Development of quantitative computed tomography lung protocols. J Thorac Imaging. 2013; 28(5):266–71. https://doi.org/10.1097/RTI.0b013e31829f6796 PMID: 23934142

43. Ley-Zaporozhan J, Ley S, Weinheimer O, Iliyushenko S, Erdugan S, Eberhardt R, et al. Quantitative analysis of emphysema in 3D using MDCT: influence of different reconstruction algorithms. Eur J Radiol. 2008; 65(2):228–34. https://doi.org/10.1016/j.ejrad.2007.03.034 PMID: 17499951

44. Wu HW, Cheng JJ, Li JY, Yin Y, Hua J, Xu JR. Pulmonary embolism detection and characterization through quantitative iodine-based material decomposition images with spectral computed tomography imaging. Invest Radiol. 2012; 47(1):85–91. https://doi.org/10.1097/RLI.0b013e31823441a1 PMID: 22107805

45. Matsumoto K, Jinzaki M, Tanami Y, Ueno A, Yamada M, Kuribayashi S. Virtual monochromatic spectral imaging with fast kilovoltage switching: improved image quality as compared with that obtained with conventional 120-kVp CT. Radiology. 2011; 259(1):257–62. https://doi.org/10.1148/radiol.11100978 PMID: 21330561